

A Unified Solution to Diverse Heterogeneities in One-shot Federated Learning

Jun Bai*

Deakin University
Melbourne, Australia
baijun@deakin.edu.au

Yiliao Song*

The University of Adelaide
Adelaide, Australia
lia.song@adelaide.edu.au

Di Wu*

University of Southern Queensland
Toowoomba, Australia
di.wu@unisq.edu.au

Atul Sajjanhar

Deakin University
Melbourne, Australia
atul.sajjanhar@deakin.edu.au

Yong Xiang

Deakin University
Melbourne, Australia
yong.xiang@deakin.edu.au

Wei Zhou

Monash University
Melbourne, Australia
wei.zhou2@monash.edu

Xiaohui Tao

University of Southern Queensland
Toowoomba, Australia
xiaohui.tao@unisq.edu.au

Yan Li

University of Southern Queensland
Toowoomba, Australia
yan.li@unisq.edu.au

Abstract

One-shot federated learning (FL) limits the communication between the server and clients to a single round, which largely decreases the privacy leakage risks in traditional FLs requiring multiple communications. However, we find existing one-shot FL frameworks are vulnerable to distributional heterogeneity due to their insufficient focus on data heterogeneity while concentrating predominantly on model heterogeneity. Filling this gap, we propose a unified, data-free, one-shot federated learning framework (FedHydra) that can effectively address both model and data heterogeneity. Rather than applying existing *value-only* learning mechanisms, a *structure-value* learning mechanism is proposed in FedHydra. Specifically, a new stratified learning *structure* is proposed to cover data heterogeneity, and the *value* of each item during computation reflects model heterogeneity. By this design, the data and model heterogeneity issues are simultaneously monitored from different aspects during learning. Consequently, FedHydra can effectively mitigate both issues by minimizing their inherent conflicts. We compared FedHydra with three SOTA baselines on four benchmark datasets. Experimental results show that our method outperforms the previous one-shot FL methods in both homogeneous and heterogeneous settings.

CCS Concepts

• **Computing methodologies** → **Distributed artificial intelligence.**

*Authors contributed equally to this research.

Permission to make digital or hard copies of all or part of this work for personal or classroom use is granted without fee provided that copies are not made or distributed for profit or commercial advantage and that copies bear this notice and the full citation on the first page. Copyrights for components of this work owned by others than the author(s) must be honored. Abstracting with credit is permitted. To copy otherwise, or republish, to post on servers or to redistribute to lists, requires prior specific permission and/or a fee. Request permissions from permissions@acm.org.

Conference acronym 'XX, June 03–05, 2018, Woodstock, NY

© 2018 Copyright held by the owner/author(s). Publication rights licensed to ACM.

ACM ISBN 978-1-4503-XXXX-X/18/06

<https://doi.org/XXXXXXXXXXXXXX>

Keywords

One-shot Federated Learning, Data Free, Heterogeneity Problems

ACM Reference Format:

Jun Bai, Yiliao Song, Di Wu, Atul Sajjanhar, Yong Xiang, Wei Zhou, Xiaohui Tao, and Yan Li. 2018. A Unified Solution to Diverse Heterogeneities in One-shot Federated Learning. In *Proceedings of Make sure to enter the correct conference title from your rights confirmation email (Conference acronym 'XX)*. ACM, New York, NY, USA, 13 pages. <https://doi.org/XXXXXXXXXXXXXX>

1 Introduction

Federated learning (FL) can promise enhanced privacy and data security via collaborative effort in training a global model across multiple clients without sharing private data [19]. Existing studies implicate two *limitations* in traditional FL, *i.e.*, **(I)** it is vulnerable to potential attacks due to its reliance on multi-round communications [10, 25, 32, 37]; **(II)** the performance will be largely impaired under heterogeneity scenarios [1, 9, 11, 20]. These issues highlight the need for heterogeneity-tolerant and short-communicated FLs to ensure privacy and efficiency across diverse and sensitive applications.

One-shot FL is proposed to overcome *limitation (I)* by limiting the communications into one-round. By this design, one-shot FLs can minimize risks associated with data sharing and communication costs while maintaining data privacy. Meanwhile, existing one-shot FLs show potential capabilities to address *limitation (II)* [4, 5, 8, 15, 36, 39]. For example, recent methods have used auxiliary public datasets [4, 5, 15, 39] or embedding client data [8] to mitigate the heterogeneity issue. Despite its potential, one-shot FL still performs poorly in highly heterogeneous scenarios, which largely prevents one-shot FL from being applied in reality [9, 20, 23, 30, 40].

To further discover the cause for low heterogeneity tolerance in existing one-shot FLs, we review the heterogeneity scenarios from *data* or *model* dimensions. *Data heterogeneity* can be presented as label heterogeneity *i.e.*, Fig. 1 (a), which arises when clients have different classes [7] or size heterogeneity *i.e.*, Fig. 1 (b), which refers to the disparity in dataset volumes across clients [6]. The label heterogeneity can skew global model performance towards more

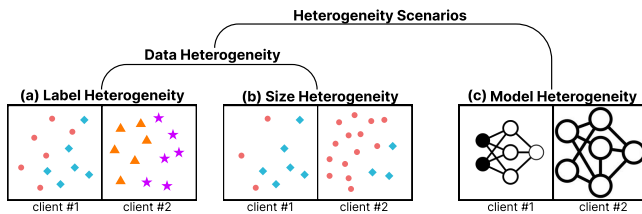


Figure 1: Illustration of heterogeneity problems (a) Label Heterogeneity, (b) Size Heterogeneity, and (c) Model Heterogeneity.

prevalent classes, while size heterogeneity leads to the problem of dominance by larger datasets. *Model heterogeneity* i.e., Fig. 1 (c) involves clients employing diverse model architectures [16].

Diverse heterogeneity scenarios might present simultaneously but existing solutions can only address heterogeneity from one dimension. For example, auxiliary public datasets are introduced to mitigate data heterogeneity [4, 5, 15, 39] but the model heterogeneity is unsolved. This will limit their application where customized models are required to meet specific needs. Recent data-free one-shot FLs, FEDCVAE-ENS and FEDCVAE-KD [8], although managing heterogeneity well, have high risks of data leakage as they directly embed the client data and upload the embedding to the server. DENSE, another data-free one-shot FL, known for its practical applicability, eliminates the need for auxiliary datasets and can accommodate model heterogeneity [36]. However, data heterogeneity remains an unaddressed challenge that weakens its performance.

To fill this gap, we propose FedHydra, a data-free one-shot FL framework that can solve data and model heterogeneity problems. Existing studies assume all clients equally contribute to the global model in the existing studies and thus apply a *value-only learning mechanisms* to aggregate heterogeneous client models on the server. However, this can not handle the data heterogeneity scenarios. To include data heterogeneity during aggregation, we propose a *structure-value learning mechanism* where the structure should be able to simulate the impact of data heterogeneity on the global model.

As the data heterogeneity must be from clients, its impact first goes through the client and then directs to the server. To mimic this client-server pathway, we propose a new *stratified structure* so that implementing the value-learning mechanism within this structure can overcome data and model heterogeneity during aggregation. In addition, the data heterogeneity is monitored by the stratified structure and the model heterogeneity is monitored by the value-learning. By this design, FedHydra can effectively mitigate data and model heterogeneity issues by minimizing their inherent conflicts.

The contributions of the proposed FedHydra are as follows: 1) A structure-value learning mechanism is proposed to simultaneously monitor data and model heterogeneity. 2) A stratified structure is proposed to mimic the pathway of the impact of data heterogeneity 3) We extensively compare FedHydra across multiple benchmark datasets under both homogeneous and heterogeneous settings. The results consistently demonstrate the superior efficacy of our method compared to state-of-the-art baselines.

2 Related Works

FL [19], introduced as a decentralized learning framework, is facing the challenge of the heterogeneity issue. Various strategies have

been developed to tackle this issue, including enhancements to the FedAvg algorithm [19] with proximal terms to control divergent updates [1, 11, 14, 16, 31] and the use of knowledge distillation (KD) to navigate parameter averaging challenges presented by non-IID data, either by utilizing auxiliary data [17, 26] or generative models [38, 40] for efficient learning across client models. Recent efforts have also aimed at optimizing client selection [29], mitigating catastrophic forgetting to safeguard against the loss of learned information [9], and broadening the applicability of client models [20]. Nevertheless, these strategies primarily cater to the traditional FL model, depending heavily on repeated communications, which contrasts sharply with the one-shot FL paradigm that restricts exchanges to a singular round, highlighting a gap in addressing statistical heterogeneity within this constrained communication context.

One-shot FL shows promising performance due to its minimal communication, which applies strategies like heuristic client selection for ensemble learning and KD techniques utilizing auxiliary datasets for aggregation [5]. Subsequent research expanded KD applications to accommodate diverse local model structures [15]. Despite achieving high accuracy, these one-shot FL methods often depend on auxiliary data, challenging their application in scenarios where data cannot be freely shared. Innovations such as dataset distillation [39] and data augmentation [27] have been explored for secure data transfer, with Zhang et al. [36] proposing a data-free KD approach leveraging a generator network trained on client model ensembles. Heinbaugh et al. [8] introduced the concepts of FEDCVAE-ENS and FEDCVAE-KD to tackle statistical heterogeneity by leveraging knowledge distillation, respectively, to enhance the efficiency of model training. However, this method manipulates the local data on clients, and the uploaded decoder may cause high risks of data leakage. Nevertheless, many one-shot FL methods struggle with or have not been tested against high statistical heterogeneity, which is the gap our proposed methods aim to fill.

In data-free KD [18], DeepInversion [34] create images by optimizing RGB pixels using cross-entropy and regularization losses, enhancing the quality of the synthesis by minimizing feature statistics in Batch Normalization (BN) layers. DAFL [2] generates images using a generator with the teacher model acting as a discriminator. ZSKT [21] generates images highlighting discrepancies between the student and teacher models to avoid overfitting in the student model. Unlike methods that select the optimal image for KD training, our strategy leverages all generated intermediate images to mitigate overfitting risks. Furthermore, although Raikward et al. [24] introduced a KD technique that utilizes random noise as a training input, it still necessitates using real images during the training process. Besides, it requires several iterative adjustments to the BN layer statistics. In contrast, our approach enables one-shot FL without needing real images during training.

3 Methodology

This section introduces the proposed FedHydra framework and the theory and algorithms of the Model Stratification and Structure-Value Learning Mechanism phases.

3.1 FedHydra: An overview

The proposed FedHydra presents a data-free one-shot FL training scheme comprising two core components: model stratification and

Algorithm 1 FedHydra Algorithm

```

1: Input: Client models  $\{F_k(\cdot)\}_{k=1}^m$  with parameters  $\{\theta^k\}_{k=1}^m$ , the
   global model  $F_g(\cdot)$  with parameter  $\theta^g$ , the Generator  $G(\cdot)$  with
   parameter  $\theta_G$ , class labels  $\{y^j\}_{j=1}^c$ , the global model training
   epochs  $T_g$  and learning rate  $\eta_g$ , and the generator training epochs
    $T_G$  and learning rate  $\eta_G$ .
2: Output: Well trained global model  $\theta^g$ 
3: procedure FedHydra():
4:   for each client model  $\theta^k$  in parallel do
5:      $\theta^k \leftarrow \text{LocalUpdate}(k)$ 
6:     Upload  $\theta^k$  to the server
7:   end for
8:   // model stratification
9:    $\bar{U}_r, \bar{U}_c \leftarrow \text{ModelStratification}(\{\theta^k\}_{k=1}^m, \theta_G, \{y^j\}_{j=1}^c)$ 
10:                                     ▶ See Algorithm 2.
11:   Initialize  $\theta^g$  and  $\theta_G$ 
12:   for each global training epoch  $t_g$  from 1 to  $T_g$  do
13:     Sample a batch of noises and labels  $\{z_i, y_i\}_{i=1}^b$ , denoted
14:     as  $\mathbf{z} = \{z_i\}_{i=1}^b$  and  $\mathbf{y} = \{y_i\}_{i=1}^b$ 
15:     // data generation
16:     for each generator training epoch  $t$  from 1 to  $T_G$  do
17:       Generate synthetic data  $\hat{\mathbf{x}} = \{\hat{x}_i\}_{i=1}^b \leftarrow G(\mathbf{z}; \theta_G^t)$ 
18:       Compute the loss  $\mathcal{L}_{Gen}$  by Eq. (16)
19:                                     ▶ See Algorithm 3 for SA computation.
20:        $\theta_G^{t+1} \leftarrow \theta_G^t - \eta_G \nabla_{\theta_G^t} \mathcal{L}_{Gen}$ 
21:     end for
22:     // model distillation
23:     Compute the loss  $\mathcal{L}_{Glo}$  by Eq. (19)
24:      $\theta_{t_g+1}^g \leftarrow \theta_{t_g}^g - \eta_g \nabla_{\theta_{t_g}^g} \mathcal{L}_{Glo}$ 
25:   end for
26:   return  $\theta^g$ 
27: end procedure

```

a structure-value learning mechanism. The latter encompasses data generation and model distillation. Within the model stratification phase, we access the classification capability of all client models across all class labels. This involves evaluating the refined weight of each client model for a particular label derived from the training loss surface of the generator, with guidance from the local model. These refined weights, serving as indicators of classification capability, are then utilized to compute the stratified aggregation (SA) for prediction logits of client models. The SA facilitates the training of both the generator and the global model.

In the structure-value learning mechanism, the data generation phase is responsible for training a generator with the SA-based guidance of client models. The synthetic data generated by this well-trained generator is subsequently employed in realizing the distillation training of the global model. Throughout the entire training process, the two phases alternate. This ensures the alignment of knowledge between synthetic and real data. In our framework, the server generates a unified global model based on client models and a single generator within a single communication round. The learning procedure is illustrated in Fig. 2, while Algorithm 1 outlines the complete training process of FedHydra.

3.2 Model Stratification

We first conduct the model stratification, aiming to evaluate the classification capability of all client models for all class labels. Specifically, we need to obtain two relative weight matrices. One weight matrix represents the guidance capability of a particular client model across all class labels, and the other represents the guidance capability for a particular class label across all client models.

Assume there are c class labels indexed by j and m clients indexed by k in the federated task. To evaluate the classification capability of one client model for a particular class j , we can allow a single client model $F_k(\theta^k)$ to separately guide the training of the Generator $G(\theta_G)$ for generating data with the same class label. In the t^{th} iteration, we can calculate the following cross-entropy (CE) loss:

$$\ell_{k,j}^t(\hat{x}_t^j, y_t^j; \theta_G) = CE(F(\hat{x}_t^j; \theta^k), y_t^j), \quad (1)$$

where \hat{x}_t^j and y_t^j denotes the generated samples and assigned labels. After the entire T_G iterations, we can obtain the corresponding loss variance denoted as $L_{k,j} = [\ell_{k,j}^1, \dots, \ell_{k,j}^t, \dots, \ell_{k,j}^{T_G}]$. Since larger loss variance and smaller minimum loss value represent the stronger guidance to the Generator from the teacher model, the guidance capability of the client model $F_k(\theta^k)$ to the class j can be defined as

$$u_{k,j} = \frac{\max(L_{k,j}) - \min(L_{k,j})}{\min(L_{k,j})}. \quad (2)$$

Based on this, we can obtain a basic guidance capability matrix with a size of $c \times m$ for all client models across all class labels as

$$U = ([u_{k,j}]_{m \times c})^T. \quad (3)$$

Each row of U showcases the guidance capability for a single class label across all client models and each column of U represents the guidance capability of a single client model across all class labels. To realize the stratified aggregation for prediction logits of client models, we need to compare the measure values in U to attain relative importance weights of guidance capability of a particular client model across all class labels as well as for a particular class label across all client models. So we first normalize each row of U to $[0, 1]$ by

$$\bar{u}_{k,j} = \frac{u_{k,j}}{\sum_{k=1}^m u_{k,j}}. \quad (4)$$

The final normalized U by row can be defined as follows:

$$\bar{U}_r = ([\bar{u}_{k,j}]_{m \times c})^T, \quad (5)$$

wherein $\sum_{k=1}^m \bar{u}_{k,j} = 1$. Each row vector of \bar{U}_r represents the stratified weights for prediction logits from all client models for a particular class sample.

Then, we normalize each column of U to $[0, 1]$ as follows:

$$\hat{u}_{k,j} = \frac{u_{k,j}}{\sum_{j=1}^c u_{k,j}}. \quad (6)$$

The final normalized U by column is defined as

$$\bar{U}_c = ([\hat{u}_{k,j}]_{m \times c})^T, \quad (7)$$

wherein $\sum_{j=1}^c \hat{u}_{k,j} = 1$. Each column vector of \bar{U}_c represents the stratified weights for prediction logits of a particular client model across all class labels. The detailed procedure for conducting the model stratification is provided in Algorithm 2.

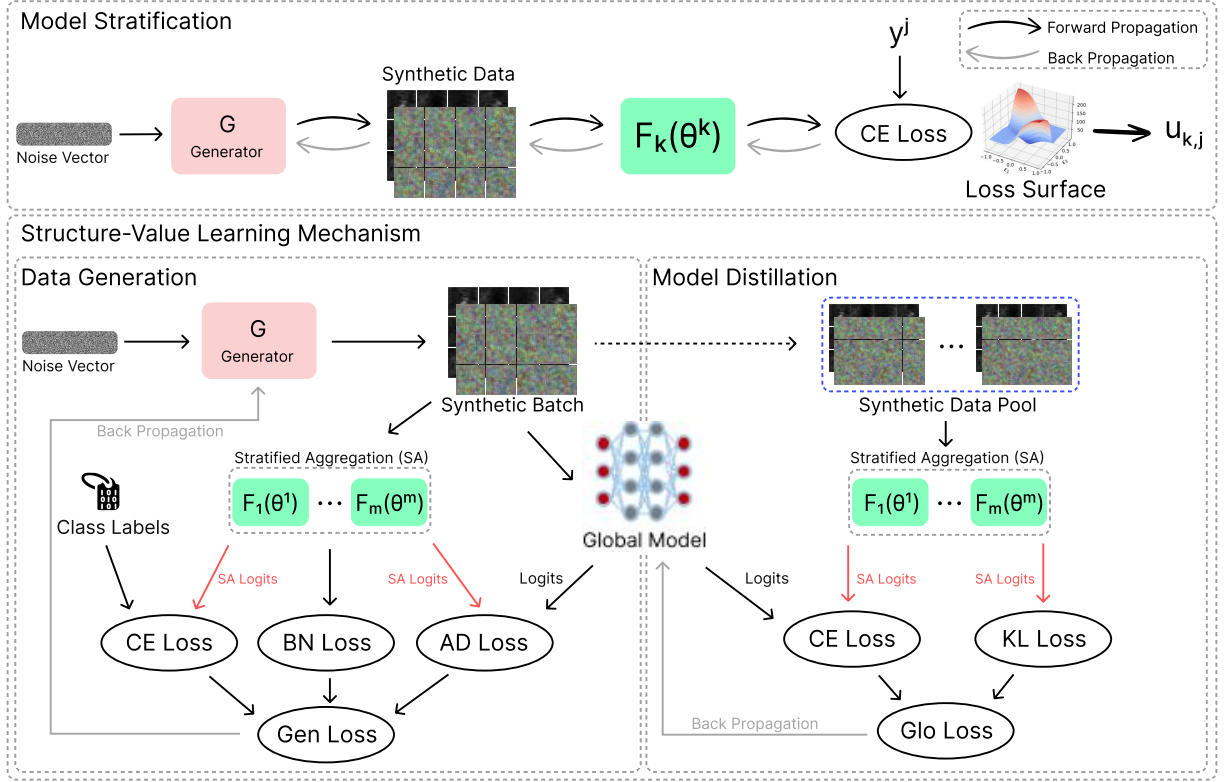


Figure 2: Illustration of the FedHydra framework.

3.3 Structure-Value Learning Mechanism

3.3.1 Stratified Aggregation. For batch-generated samples by Generator and assigned target labels $(\mathbf{x}, \mathbf{y}) = \{x_i, y_i^j\}_{i=1}^b$ with size b , each client model on \mathbf{x} will output its batch prediction logits denoted as $P_k = F_k(\mathbf{x}; \theta^k)$ with size $b \times c$.

Based on Eq. (7), we first conduct an in-model weighted batch prediction logits \hat{P}_k for each P_k by

$$\hat{P}_k = P_k \odot (\mathbf{I}_{b \times 1} \times (\bar{U}_c(:, k))^T), \quad (8)$$

wherein \odot means the Hadamard product, $\mathbf{I}_{b \times 1}$ represents a column vector of size $b \times 1$ filled with ones, and $\bar{U}_c(:, k)$ denotes the k^{th} column of \bar{U}_c . Then, we can obtain in-model weighted prediction logits set P^i for the i^{th} in-batch sample across all client models as below:

$$P^i = \begin{bmatrix} \hat{P}_1(i, :) \\ \vdots \\ \hat{P}_k(i, :) \\ \vdots \\ \hat{P}_m(i, :) \end{bmatrix}_{m \times c} \quad (i = 1, 2, \dots, b), \quad (9)$$

wherein $\hat{P}_k(i, :)$ means the i^{th} row of \hat{P}_k . Subsequently, based on Eq. (5), the weight set for the guidance capability of all client

models on batch samples can be calculated by

$$V = \begin{bmatrix} \bar{U}_r(\mathbf{y}(1), :) \\ \vdots \\ \bar{U}_r(\mathbf{y}(i), :) \\ \vdots \\ \bar{U}_r(\mathbf{y}(b), :) \end{bmatrix}_{b \times m}, \quad (10)$$

wherein $\mathbf{y}(i)$ denotes the i^{th} target class label and $\bar{U}_r(\mathbf{y}(i), :)$ means the $\mathbf{y}(i)^{\text{th}}$ row of \bar{U}_r . Combining Eq. (9) and Eq. (10), the inter-model weighted batch prediction logits P can be calculated by

$$P = \begin{bmatrix} V(1, :) \times P^1 \\ \vdots \\ V(i, :) \times P^i \\ \vdots \\ V(b, :) \times P^b \end{bmatrix}_{b \times c}, \quad (11)$$

wherein $V(i, :)$ represents the i^{th} row of V , and P is the final ensemble prediction logits output, termed **Stratified Aggregation (SA)**. The specific computation process is summarized in Algorithm 3.

3.3.2 Data Generation. In this phase, our objective is to train a generator guided by client models to generate synthetic data with a similar distribution that closely matches the distribution of the group client data. Inspired by [36], we consider the generator training from three aspects.

Algorithm 2 Model Stratification

```

1: Input: Client models  $\{F_k(\theta^k)\}_{k=1}^m$ , the Generator  $G(\theta_G)$  and
   class labels  $\{y^j\}_{j=1}^c$ 
2: Output: Stratified weight matrices  $\bar{U}_r$  and  $\bar{U}_c$ 
3: procedure ModelStratification( $\{\theta^k\}_{k=1}^m, \theta_G, \{y^j\}_{j=1}^c$ ):
4:   for each client model  $\theta^k, k$  from 1 to  $m$  do
5:     for each class label  $y^j, j$  from 1 to  $c$  do
6:       Initialize the Generator parameter  $\theta_G$ 
7:       Sample a batch of noise vectors and labels
          $\{z_i, y_i^j\}_{i=1}^b$ , denoted as  $\mathbf{z} = \{z_i\}_{i=1}^b$  and  $\mathbf{y} = \{y_i^j\}_{i=1}^b$ 
8:       // evaluate the guidance capability by Generator
9:       for each training epoch  $t$  from 1 to  $T_G$  do
10:         $\hat{\mathbf{x}} = \{\hat{x}_i\}_{i=1}^b \leftarrow G(\mathbf{z}; \theta_G^t)$ 
11:         $\ell_{k,j}^t \leftarrow CE(F_k(\hat{\mathbf{x}}; \theta^k), \mathbf{y})$ 
12:         $L_{k,j} \leftarrow \ell_{k,j}^t$ 
13:         $\theta_G^{t+1} \leftarrow \theta_G^t - \eta_G \nabla_{\theta_G} \ell_{k,j}^t$ 
14:      end for
15:      Compute  $u_{k,j}$  based on  $L_{k,j}$  by Eq. (2)
16:       $U \leftarrow u_{k,j}$ 
17:    end for
18:  end for
19:  Compute  $\bar{U}_r$  and  $\bar{U}_c$  by Eq. (5) and Eq. (7) based on  $U$ 
20:  return  $\bar{U}_r$  and  $\bar{U}_c$ 
21: end procedure

```

We first compute the SA prediction logits with Algorithm 3 for a batch-generated data $\hat{\mathbf{x}} = G(\mathbf{z}; \theta_G)$ and their assigned labels \mathbf{y} , as follows:

$$P = \text{SA}(\hat{\mathbf{x}}, \mathbf{y}, \{\theta^k\}_{k=1}^m), \quad (12)$$

where P is our proposed SA logits. Then, to ensure the distribution similarity between synthetic data and real client data, we minimize the cross-entropy (CE) loss between P and \mathbf{y} , defined in Eq. (13), in the training objective function of the generator.

$$\mathcal{L}_{CE}(\hat{\mathbf{x}}, \mathbf{y}; \theta_G) = CE(P, \mathbf{y}). \quad (13)$$

Second, Batch Normalization (BN) loss introduced in [36] is also employed to increase the stability of generator training, defined as follows:

$$\mathcal{L}_{BN}(\hat{\mathbf{x}}; \theta_G) = \frac{1}{m} \sum_{k=1}^m \sum_l \left(\|\mu_l(\hat{\mathbf{x}}) - \mu_{k,l}(\hat{\mathbf{x}})\| + \|\sigma_l^2(\hat{\mathbf{x}}) - \sigma_{k,l}^2(\hat{\mathbf{x}})\| \right), \quad (14)$$

where $\mu_l(\hat{\mathbf{x}})$ and $\sigma_l^2(\hat{\mathbf{x}})$ are the batch-wise mean and variance of hidden features from the l^{th} BN layer of the generator, $\mu_{k,l}(\hat{\mathbf{x}})$ and $\sigma_{k,l}^2(\hat{\mathbf{x}})$ are the mean and variance of the l^{th} BN layer of the k^{th} client model.

Third, to increase the diversity of generated data, an adversarial distillation (AD) loss is considered to maximize the discrepancy between SA logits and prediction logits of the global model, defined as follows:

Algorithm 3 Stratified Aggregation (SA)

```

1: Input: Client models  $\{F_k(\theta^k)\}_{k=1}^m$ , two weight matrices  $\bar{U}_r$  and
    $\bar{U}_c$  from model stratification, and synthetic batch data  $(\hat{\mathbf{x}}, \mathbf{y}) =$ 
    $\{\mathbf{x}_i, \mathbf{y}_i\}_{i=1}^b$ 
2: Output: weighted batch prediction logits matrix  $P$ 
3: procedure SA( $\{\theta^k\}_{k=1}^m, \bar{U}_r, \bar{U}_c, (\hat{\mathbf{x}}, \mathbf{y})$ )
4:   for each client model  $\theta^k, k$  from 1 to  $m$  do
5:      $P_k \leftarrow F_k(\mathbf{x}; \theta^k)$ 
6:     Compute in-model weighted prediction logits  $\hat{P}_k$  based
       on  $P_k$  and  $\bar{U}_c$  by Eq. (8)
7:   end for
8:   Compute inter-model weighted prediction logits  $P$  based on
      $\{\hat{P}_k\}_{k=1}^m$  and  $\bar{U}_r$  by Eq. (9), (10), and (11)
9:   return  $P$ 
10: end procedure

```

$$\mathcal{L}_{AD}(\hat{\mathbf{x}}, \mathbf{y}; \theta_G) = -KL(P, F_g(\hat{\mathbf{x}}; \theta^g)), \quad (15)$$

where $F_g(\cdot)$ and θ^g denote the global model and its parameter. Therefore, the final generator training loss is defined by combining the above three loss terms, as follows:

$$\mathcal{L}_{Gen}(\hat{\mathbf{x}}, \mathbf{y}; \theta_G) = \mathcal{L}_{CE}(\hat{\mathbf{x}}, \mathbf{y}; \theta_G) + \lambda_1 \mathcal{L}_{BN}(\hat{\mathbf{x}}; \theta_G) + \lambda_2 \mathcal{L}_{AD}(\hat{\mathbf{x}}, \mathbf{y}; \theta_G), \quad (16)$$

where λ_1 and λ_2 are adjustable parameters.

3.3.3 Model Distillation. Based on the synthetic data produced in the data generation phase, we design a new model distillation scheme to train our global model with knowledge distillation techniques.

We consider the two loss terms in the training objective function of the global model. First, we use the KL loss between the SA logits and prediction logits of the global model to distill the knowledge from client models to the global model, defined as

$$\mathcal{L}_{KL}(\hat{\mathbf{x}}, \mathbf{y}; \theta^g) = KL(P, F_g(\hat{\mathbf{x}}; \theta^g)). \quad (17)$$

To achieve efficient and stable model distillation, ensuring consistent prediction labels between the ensemble client models and the global model is crucial, especially considering the potential deviation between synthetic and real data. So, we introduce the following CE loss, defined as:

$$\mathcal{L}_{\widehat{CE}}(\hat{\mathbf{x}}, \mathbf{y}; \theta^g) = CE(F_g(\hat{\mathbf{x}}; \theta^g), H[P]), \quad (18)$$

where $H[\cdot]$ represents to obtain the hard label of prediction logits. Therefore, by combining the above two loss terms, the final training loss function for realizing model distillation is defined as follows:

$$\mathcal{L}_{Glo}(\hat{\mathbf{x}}, \mathbf{y}; \theta^g) = \mathcal{L}_{KL}(\hat{\mathbf{x}}, \mathbf{y}; \theta^g) + \beta \mathcal{L}_{\widehat{CE}}(\hat{\mathbf{x}}, \mathbf{y}; \theta^g), \quad (19)$$

where β is an adjustable parameter.

4 Experiments

4.1 Setup

4.1.1 Datasets. Our evaluation experiments utilize four datasets: MNIST [13], FashionMNIST [33], SVHN [22], and CIFAR10 [12].

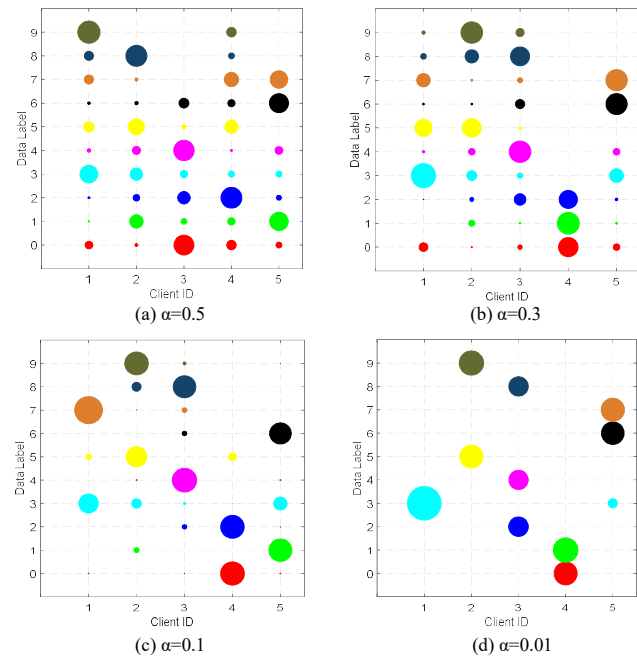


Figure 3: Visualization of heterogeneous distributions of client data characterized by four diverse α values, with MNIST used as an illustration. The horizontal axis denotes the client ID, while the vertical axis represents the class label. Each circle’s size corresponds to the number of data samples linked to a specific class, and circles of identical color denote the same class label.

MNIST comprises 60,000 training images and 10,000 testing images of handwritten digits, each with a size of 28x28 pixels. FashionMNIST provides a more challenging fashion item classification dataset, with the same quantities of image and label and size specifications as MNIST. SVHN consists of over 600,000 color images of house numbers extracted from Google Street View, suitable for digit recognition tasks. Lastly, CIFAR10 comprises 60,000 32x32 color images across 10 object classes, with 50,000 images for training and 10,000 for testing.

4.1.2 Client Data Distribution. We adopt the Dirichlet distribution method ($Dir(\alpha)$) in [35] to simulate diverse client data distributions in practical FL scenarios, as shown in Fig. 3. Adjusting the parameter α allows us to modify the level of data heterogeneity: a lower α results in more pronounced heterogeneity in the data distribution, while a higher α results in a homogeneous data distribution. We establish $\alpha = 0.5$ by default to initiate this process.

4.1.3 Baselines. Since the proposed method aims to solve the heterogeneity problem in one-shot FL, we omit the comparison with some approaches, like FedBE [3], and FedGen [40], which need to download auxiliary models or datasets. In addition, methods such as FedProx [16], FedNova [31], and Scaffold [11] are also not considered because regularization-based methods are not designed for one-shot FL. Furthermore, we are not comparing with FEDCVAE [8], which directly embeds the data on the client side and uploads it to the server without model training on the client. Therefore, We

choose three State-of-the-art (SOTA) baselines: FedAvg [19], FedDF [17], and DENSE [36].

4.1.4 Configurations. In our FL setup, we set the client number $m = 5$. For the client model training, we employ the SGD optimizer with learning rate $\eta = 0.01$, while setting the local epochs and batch size as $B = 128$ and $E = 200$, respectively. On the server side, we utilize the Adam optimizer with learning rate $\eta_G = 0.001$ to train the generator. This generator, characterized by adjustable parameters $\lambda_1 = 1.0, \lambda_2 = 0.5$, undergoes training for $T_G = 30$ rounds to generate batch examples. For the distillation training of the global model, we set the training epochs to $T_g = 200$ and the learning rate to $\eta_g = 0.01$, with SGD serving as the optimizer.

4.2 Evaluation

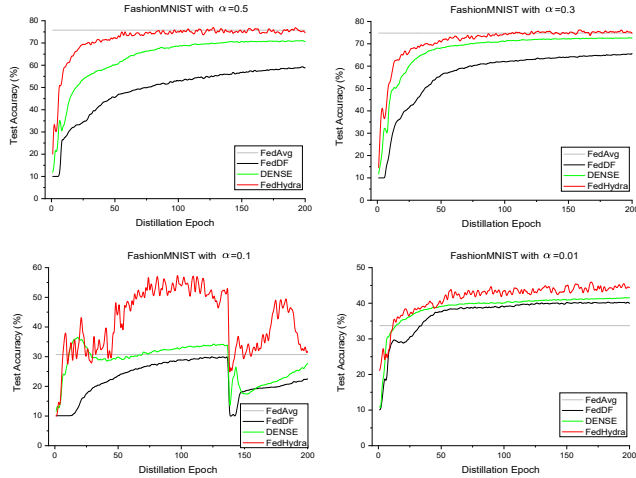
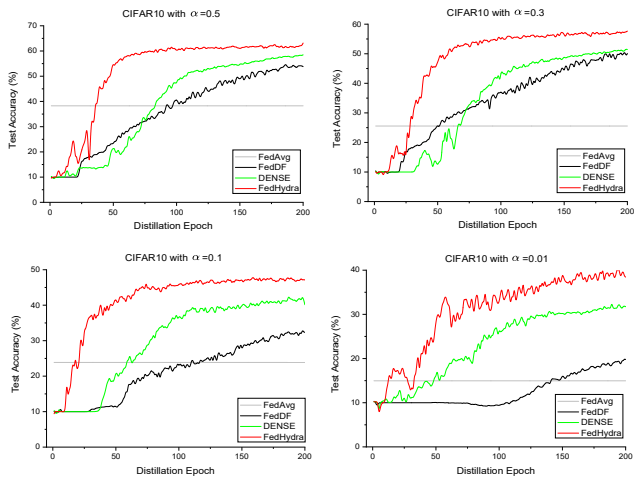
We report the key experimental results in this section, and more experiment results are reported in the appendix within the submitted Supplementary Material.

4.2.1 Performance Overview. Table 1 presents the testing performance on FedHydra and comparative methods over four datasets with different α of client data distribution, which varies from 0.5 to 0.01 wherein $\alpha = 0.01$ indicates an extreme data heterogeneity situation. The results show that our FedHydra achieves the highest accuracy across all the data heterogeneity settings with all the datasets. Specifically, all the methods perform well on the MNIST dataset because of less data heterogeneity when $\alpha = 0.5$. Our FedHydra outperforms the baseline FedAvg by 3.99%, FedDF by 6.85%, and DENSE by 7.22%, respectively. Furthermore, When the data heterogeneity increases, we observe that FedAvg decreases dramatically from 81.89% to 69.89% when $\alpha = 0.3$, then further down to 25.96% when $\alpha = 0.1$, the accuracy only achieved 10.10% when $\alpha = 0.01$ under an extremely data heterogeneity situation. Other methods like FedDF and DENSE show similar trends when the data heterogeneity increases. However, our FedHydra shows robustness under data heterogeneity situations, which outperforms the second-best method, DENSE, by 7.22% when $\alpha = 0.3$, 23.24% when $\alpha = 0.1$, and 27.66% when $\alpha = 0.01$. This is because FedAvg averages the uploaded parameters from the clients, which causes less robustness when data heterogeneity happens. FedDF requires prior data with the average ensemble logits from the uploaded models to process the model distillation, similar to the reason for DENSE. The averaged ensemble logits could not guide the generator to generate the synthetic data by specific labels when data heterogeneity increases.

The result patterns are similar on other datasets, including FashionMNIST, SVHN, and CIFAR10. Our FedHydra outperforms the second-highest by 1.44%, 1.58%, 12.24% and 4.37%, and achieved 77.20%, 76.39%, 50.84% and 46.02% from $\alpha = 0.5$ to 0.01 on FashionMNIST, respectively. On SVHN, FedHydra outperforms the second-highest by 2.19%, 1.96%, 7.73% and 9.01%, and achieved 82.39%, 82.96%, 62.08% and 30.95% from $\alpha = 0.5$ to 0.01. In addition, FedHydra also outperforms the second-highest by 4.67%, 6.09%, 5.56% and 7.94%, and achieved 63.15%, 57.66%, 48.12% and 40.63% from $\alpha = 0.5$ to 0.01 on CIFAR10, respectively. Therefore, the results prove that the proposed FedHydra significantly outperforms the SOTA baseline methods, further illustrating the superior performance of FedHydra in a data heterogeneity environment.

Table 1: Top-1 test accuracy achieved by FedAvg, FedDF, DENSE, and FedHydra over various datasets with varying α .

Dataset	MNIST				FashionMNIST				SVHN				CIFAR10			
	$\alpha=0.5$	$\alpha=0.3$	$\alpha=0.1$	$\alpha=0.01$	$\alpha=0.5$	$\alpha=0.3$	$\alpha=0.1$	$\alpha=0.01$	$\alpha=0.5$	$\alpha=0.3$	$\alpha=0.1$	$\alpha=0.01$	$\alpha=0.5$	$\alpha=0.3$	$\alpha=0.1$	$\alpha=0.01$
FedAvg	81.89	69.89	25.96	10.10	75.76	74.81	30.71	33.71	59.94	64.64	31.46	21.94	38.26	25.54	23.87	14.96
FedDF	78.23	73.59	31.52	10.10	59.38	65.61	32.11	40.36	80.20	81.00	54.35	7.59	54.81	50.82	33.06	19.91
DENSE	77.86	76.78	36.73	11.17	71.14	72.79	38.24	41.65	79.44	78.81	53.69	7.75	58.48	51.57	42.56	32.69
FedHydra (ours)	85.08	85.16	59.97	38.83	77.20	76.39	50.48	46.02	82.39	82.96	62.08	30.95	63.15	57.66	48.12	40.63

**Figure 4: Test accuracy versus distillation epoch over FashionMNIST with $\alpha = \{0.5, 0.3, 0.1, 0.01\}$.****Figure 5: Test accuracy versus distillation epoch over CIFAR10 with $\alpha = \{0.5, 0.3, 0.1, 0.01\}$.**

Further experiments show the impact of accuracy versus model distillation epochs over four datasets. The corresponding test accuracy curves in each distillation epoch are provided in Fig. 4 and 5, respectively. In Fig. 4, FedHydra significantly outperforms the SOTA baseline methods after 25 epochs, especially when $\alpha \leq 0.3$. In Fig. 5, FedHydra demonstrates dominant capabilities on the CIFAR10 dataset, significantly outperforming the SOTA baseline methods from 25 epochs to 200 with $\alpha = \{0.5, 0.3, 0.1, 0.01\}$.

4.2.2 Impact of Stratified Aggregation. DENSE employs a simple averaging ensemble to aggregate the output logits from client models. This means that the averaging ensemble equally treats the classification capability of all client models on diverse class samples. However, different client models may exhibit varying classification capabilities across different class examples, especially in FL settings with data heterogeneity. Hence, our FedHydra initially evaluates the stratified weights of classification capabilities among various client models across diverse class labels. These weights are then applied to the prediction logits of client models to achieve stratified aggregation, which guides the structure-value learning mechanism.

To validate the effectiveness of stratified aggregation in heterogeneous federated data distributions, we designed a more extreme data distribution scenario with only two disjoint class samples per client, termed **2c/c**. Also, taking MNIST with **2c/c** distribution as an example, Fig. 6 (a) illustrates the data distribution across five clients in the **2c/c** case. Following this federated client data distribution, each updated client model exhibits strong classification capability solely on examples belonging to its exclusively possessed two class labels. This alignment is well-reflected in the stratified weight distributions, evaluated by model stratification, of the classification capability of the five client models across the ten class labels, as depicted in Fig. 6 (b). For instance, important classification weights of client 1 for class labels 0 and 1 are 0.9594% and 0.9797%, respectively, while weights for other class labels are nearly zero. Hence, our model stratification accurately assesses the classification capabilities of client models.

Table 2 shows the top-1 test accuracy on four datasets with **2c/c** distribution. Under the extreme data distribution case, FedHydra still shows the dominant performance over the SOTA baseline methods by overtaking the second-highest method by 20.31%, 2.33%, 8.58% and 7.73%, which achieves 40.81%, 39.06%, 50.61% and 39.09% on MNIST, FashionMNIST, SVHN, and CIFAR10, respectively. FedDF and DENSE are relatively lower than FedAvg on simple datasets under **2c/c** distribution such as MNIST and FashionMNIST because averaging ensemble logits will fail to provide valuable guidance for data generation and model distillation. However, due to the model parameter sensitivity to complicated classification tasks, FedAvg shows poor performance on complex datasets, such as SVHN and CIFAR10. The results prove that our FedHydra is robust under **2c/c** distribution. Perceptive test accuracy variations are plotted in Fig. 7. The results show that our FedHydra outperforms all the other methods over four datasets under **2c/c** distribution.

Furthermore, we compare the test accuracy of the averaging ensemble (**AE**) from DENSE and our stratified aggregation (**SA**) over four datasets, as shown in Fig. 8. The results indicate that our **SA** is much higher than **AE** in every numerical α , including **2c/c**. **AE** can reach 20.00% less than **SA** when $\alpha = 0.5$ and 0.3, where the degree of data heterogeneity is not that high. However, when $\alpha = 0.1$, **AE**

Table 2: Top-1 test accuracy achieved by FedAvg, FedDF, DENSE, and FedHydra over various datasets with 2c/c distribution.

Dataset	MNIST	FashionMNIST	SVHN	CIFAR10
FedAvg	20.50	36.73	26.68	9.22
FedDF	13.38	15.33	42.03	17.43
DENSE	15.58	22.31	41.38	31.36
FedHydra (ours)	40.81	39.06	50.61	39.09

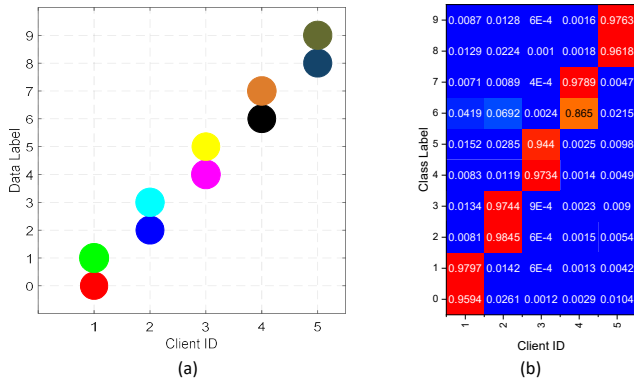


Figure 6: Visualization of stratified aggregation. (a) 2c/c data distribution across five clients using MNIST as an example. (b) The weight distribution of evaluated classification capability for five client models on ten class labels.

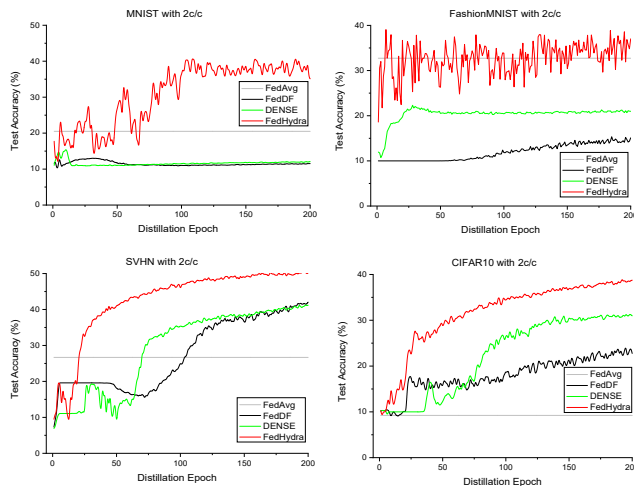


Figure 7: Test accuracy versus distillation epoch over diverse datasets with 2c/c distribution.

decreases greatly from 81.75% to 37.41% on MNIST, for example. The gap is accompanied by the increased degree of data heterogeneity, which reaches the largest gap when $\alpha = 0.01$, the degree of data heterogeneity $\alpha = 0.01$ is higher than 2c/c because $\alpha = 0.01$ represents both label and size heterogeneity. In contrast, 2c/c size are equal.

4.2.3 Impact of Stratified Aggregation Guided Model Distillation. We demonstrate the impact of our SA-guided model distillation

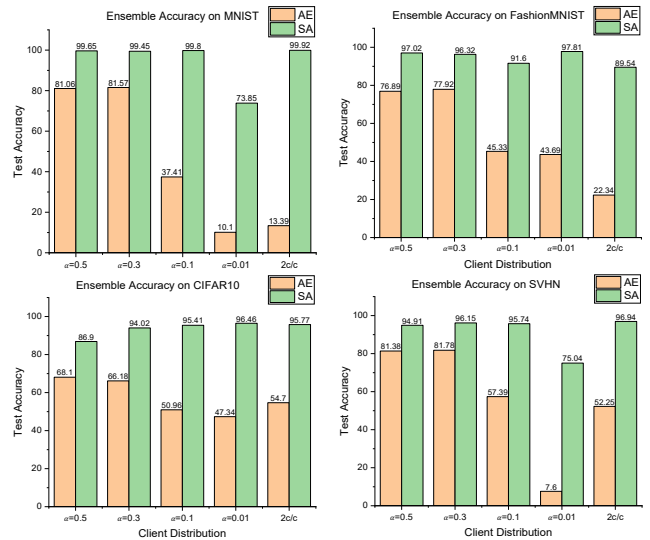


Figure 8: Test accuracy achieved by averaging ensemble (AE) and our stratified aggregation (SA) over four datasets with varying client data distributions.

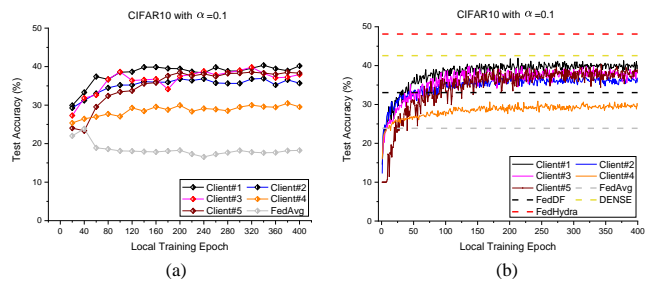


Figure 9: (a) Test accuracy of FedAvg and client models across local training epochs $E = 20, 40, 60, \dots, 400$. (b) Local training accuracy of different clients. The dotted lines represent the top-1 test accuracy achieved by FedAvg, FedDF, DENSE, and our FedHydra.

by comparing it with FedAvg, FedDF, and DENSE. Taking CIFAR10 with $\alpha = 0.1$ as an example, the results are plotted in Fig. 9. Fig. 9 (a) shows the results of the global model and local models across different local training epochs $E = \{40, 80, 120, \dots, 400\}$. The global model achieves the best performance around 24.00% when $E = 40$. This is because of the mismatch in optimization goals when dealing with data heterogeneity, resulting in weight divergence. However, Fig. 9 (b) represents the FedAvg, FedDF, DENSE, and FedHydra results ranging E from 0 to 400. FedHydra outperforms DENSE and each client model, while FedAvg performance is under client models. The results prove that SA-guided model distillation is robust under data heterogeneity while SA-guided model distillation harms the distillation performance.

4.2.4 Performance in FL Model Heterogeneity. Our proposed FedHydra can simultaneously adapt to data heterogeneity and model heterogeneity. We design five different client models, including GoogleNet, ResNet18, two simple CNNs, and LeNet, for local training on CIFAR10 by varying α values in $\{0.01, 0.1, 0.3, 0.5\}$ to evaluate the performance under both model and data heterogeneity. We choose ResNet18 as the global model on the server side. FedAvg

Table 3: Top-1 test accuracy achieved by FedDF, DENSE, and FedHydra over CIFAR10 with personalized client models.

Data Distribution	Personalized Client Model					Server (ResNet18)		
	GoogLeNet	ResNet18	CNN1	CNN2	LeNet	FedDF	DENSE	FedHydra
$\alpha=0.01$	26.68	28.78	26.71	19.28	10.00	22.25	18.67	30.51
$\alpha=0.1$	37.36	36.63	35.60	30.41	28.77	27.39	26.43	30.90
$\alpha=0.3$	46.41	55.49	45.78	47.98	33.47	46.96	44.54	48.80
$\alpha=0.5$	49.33	61.08	47.65	54.14	48.25	56.27	51.29	59.23

does not support model heterogeneity. Thus, we compare our FedHydra with FedDF and DENSE. Table 3 summarises the results of different models over CIFAR10 under both data and model heterogeneity settings. FedHydra outperforms the other methods on the server, which achieves 59.23% overtaking FedDF by 2.96%. However, by the decrease of α , both FedDF and DENSE drop dramatically from 56.27% to 22.25% and 51.29% to 18.67% when $\alpha = 0.01$. FedHydra still promises robustness in model and data heterogeneity, achieving 30.51%.

5 Conclusion

We propose FedHydra, a unified data-free one-shot federated learning framework designed to effectively address both data and model heterogeneity. FedHydra differentiates itself by employing a structure-value learning mechanism instead of the conventional value-only approach. It incorporates a newly devised stratified learning structure that accounts for data heterogeneity, and each learning item included in this structure reflects model heterogeneity. This innovative design allows for the concurrent management of data and model heterogeneity, enabling FedHydra to efficiently alleviate challenges posed by both heterogeneity. Comparative evaluations of FedHydra against SOTA baselines across four benchmark datasets demonstrate its superior performance in both homogeneous and heterogeneous settings, outstripping previous one-shot FL methodologies.

References

- [1] Durmus Alp Emre Acar, Yue Zhao, Ramon Matas, Matthew Mattina, Paul Whatmough, and Venkatesh Saligrama. 2020. Federated Learning Based on Dynamic Regularization. In *International Conference on Learning Representations*.
- [2] Hanjing Chen, Yunhe Wang, Chang Xu, Zhaohui Yang, Chuanjian Liu, Boxin Shi, Chunjing Xu, Chao Xu, and Qi Tian. 2019. Data-free learning of student networks. In *Proceedings of the IEEE/CVF international conference on computer vision*. 3514–3522.
- [3] Hong-You Chen and Wei-Lun Chao. 2020. Fedbe: Making bayesian model ensemble applicable to federated learning. *arXiv preprint arXiv:2009.01974* (2020).
- [4] Don Kurian Dennis, Tian Li, and Virginia Smith. 2021. Heterogeneity for the win: One-shot federated clustering. In *International Conference on Machine Learning*. PMLR, 2611–2620.
- [5] Neel Guha, Ameet Talwalkar, and Virginia Smith. 2019. One-shot federated learning. *arXiv preprint arXiv:1902.11175* (2019).
- [6] Haibo He and Edwardo A Garcia. 2009. Learning from imbalanced data. *IEEE Transactions on knowledge and data engineering* 21, 9 (2009), 1263–1284.
- [7] Jingrui He. 2017. Learning from Data Heterogeneity: Algorithms and Applications. In *IJCAI*. 5126–5130.
- [8] Clare Elizabeth Heinbaugh, Emilio Luz-Ricca, and Huajie Shao. 2022. Data-free one-shot federated learning under very high statistical heterogeneity. In *The Eleventh International Conference on Learning Representations*.
- [9] Wenke Huang, Mang Ye, and Bo Du. 2022. Learn from others and be yourself in heterogeneous federated learning. In *Proceedings of the IEEE/CVF Conference on Computer Vision and Pattern Recognition*. 10143–10153.
- [10] Malhar S Jere, Tyler Farnan, and Farinaz Koushanfar. 2020. A taxonomy of attacks on federated learning. *IEEE Security & Privacy* 19, 2 (2020), 20–28.
- [11] Sai Praneeth Karimireddy, Satyen Kale, Mehryar Mohri, Sashank Reddi, Sebastian Stich, and Ananda Theertha Suresh. 2020. Scaffold: Stochastic controlled averaging for federated learning. In *International conference on machine learning*. PMLR, 5132–5143.
- [12] Alex Krizhevsky, Geoffrey Hinton, et al. 2009. Learning multiple layers of features from tiny images. (2009).
- [13] Yann LeCun, Léon Bottou, Yoshua Bengio, and Patrick Haffner. 1998. Gradient-based learning applied to document recognition. *Proc. IEEE* 86, 11 (1998), 2278–2324.
- [14] Qinbin Li, Bingsheng He, and Dawn Song. 2021. Model-contrastive federated learning. In *Proceedings of the IEEE/CVF conference on computer vision and pattern recognition*. 10713–10722.
- [15] Qinbin Li, Bingsheng He, and Dawn Song. 2021. Practical One-Shot Federated Learning for Cross-Silo Setting. In *Proceedings of the Thirtieth International Joint Conference on Artificial Intelligence, IJCAI-21*. International Joint Conferences on Artificial Intelligence Organization, 1484–1490.
- [16] Tian Li, Anit Kumar Sahu, Manzil Zaheer, Maziar Sanjabi, Ameet Talwalkar, and Virginia Smith. 2020. Federated optimization in heterogeneous networks. *Proceedings of Machine Learning and Systems 2* (2020), 429–450.
- [17] Tao Lin, Lingjing Kong, Sebastian U Stich, and Martin Jaggi. 2020. Ensemble distillation for robust model fusion in federated learning. *Advances in Neural Information Processing Systems* 33 (2020), 2351–2363.
- [18] Yang Liu, Wei Zhang, Jun Wang, and Jianyong Wang. 2021. Data-free knowledge transfer: A survey. *arXiv preprint arXiv:2112.15278* (2021).
- [19] Brendan McMahan, Eider Moore, Daniel Ramage, Seth Hampson, and Blaise Aguera y Arcas. 2017. Communication-efficient learning of deep networks from decentralized data. In *Artificial intelligence and statistics*. PMLR, 1273–1282.
- [20] Matias Mendieta, Taojiannan Yang, Pu Wang, Minwoo Lee, Zhengming Ding, and Chen Chen. 2022. Local learning matters: Rethinking data heterogeneity in federated learning. In *Proceedings of the IEEE/CVF Conference on Computer Vision and Pattern Recognition*. 8397–8406.
- [21] Paul Micaelli and Amos J Storkey. 2019. Zero-shot knowledge transfer via adversarial belief matching. *Advances in Neural Information Processing Systems* 32 (2019).
- [22] Yuval Netzer, Tao Wang, Adam Coates, Alessandro Bissacco, Baolin Wu, Andrew Y Ng, et al. 2011. Reading digits in natural images with unsupervised feature learning. In *NIPS workshop on deep learning and unsupervised feature learning*, Vol. 2011. Granada, Spain, 7.
- [23] Liangqiong Qu, Yuyin Zhou, Paul Pu Liang, Yingda Xia, Feifei Wang, Ehsan Adeli, Li Fei-Fei, and Daniel Rubin. 2022. Rethinking architecture design for tackling data heterogeneity in federated learning. In *Proceedings of the IEEE/CVF conference on computer vision and pattern recognition*. 10061–10071.
- [24] Piyush Raikwar and Deepak Mishra. 2022. Discovering and overcoming limitations of noise-engineered data-free knowledge distillation. *Advances in Neural Information Processing Systems* 35 (2022), 4902–4912.
- [25] Bosen Rao, Jiale Zhang, Di Wu, Chengcheng Zhu, Xiaobing Sun, and Bing Chen. 2024. Privacy Inference Attack and Defense in Centralized and Federated Learning: A Comprehensive Survey. *IEEE Transactions on Artificial Intelligence* (2024), 1–22. <https://doi.org/10.1109/TAI.2024.3363670>
- [26] Felix Sattler, Tim Korjakow, Roman Rischke, and Wojciech Samek. 2021. Fedaux: Leveraging unlabeled auxiliary data in federated learning. *IEEE Transactions on Neural Networks and Learning Systems* 34, 9 (2021), 5531–5543.
- [27] MyungJae Shin, Chihoon Hwang, Joongheon Kim, Jihong Park, Mehdi Bennis, and Seong-Lyun Kim. 2020. Xor mixup: Privacy-preserving data augmentation for one-shot federated learning. *arXiv preprint arXiv:2006.05148* (2020).
- [28] Sidak Pal Singh and Martin Jaggi. 2020. Model fusion via optimal transport. *Advances in Neural Information Processing Systems* 33 (2020), 22045–22055.
- [29] Minxue Tang, Xuefei Ning, Yitu Wang, Jingwei Sun, Yu Wang, Hai Li, and Yiran Chen. 2022. FedCor: Correlation-based active client selection strategy for heterogeneous federated learning. In *Proceedings of the IEEE/CVF Conference on Computer Vision and Pattern Recognition*. 10102–10111.
- [30] Zhenheng Tang, Yonggang Zhang, Shaohuai Shi, Xin He, Bo Han, and Xiaowen Chu. 2022. Virtual homogeneity learning: Defending against data heterogeneity in federated learning. In *International Conference on Machine Learning*. PMLR, 21111–21132.
- [31] Jianyu Wang, Qinghua Liu, Hao Liang, Gauri Joshi, and H Vincent Poor. 2020. Tackling the objective inconsistency problem in heterogeneous federated optimization. *Advances in neural information processing systems* 33 (2020), 7611–7623.
- [32] Di Wu, Jun Bai, Yiliao Song, Junjun Chen, Wei Zhou, Yong Xiang, and Atul Sajjanhar. 2023. FedInverse: Evaluating Privacy Leakage in Federated Learning. In *The Twelfth International Conference on Learning Representations*.
- [33] Han Xiao, Kashif Rasul, and Roland Vollgraf. 2017. Fashion-mnist: a novel image dataset for benchmarking machine learning algorithms. *arXiv preprint arXiv:1708.07747* (2017).
- [34] Hongxu Yin, Pavlo Molchanov, Jose M Alvarez, Zhizhong Li, Arun Mallya, Derek Hoiem, Niraj K Jha, and Jan Kautz. 2020. Dreaming to distill: Data-free knowledge transfer via deepinversion. In *Proceedings of the IEEE/CVF Conference on Computer Vision and Pattern Recognition*. 8715–8724.

- [35] Mikhail Yurochkin, Mayank Agarwal, Soumya Ghosh, Kristjan Greenewald, Nghia Hoang, and Yasaman Khazaeni. 2019. Bayesian nonparametric federated learning of neural networks. In *International conference on machine learning*. PMLR, 7252–7261.
- [36] Jie Zhang, Chen Chen, Bo Li, Lingjuan Lyu, Shuang Wu, Shouhong Ding, Chunhua Shen, and Chao Wu. 2022. Dense: Data-free one-shot federated learning. *Advances in Neural Information Processing Systems* 35 (2022), 21414–21428.
- [37] Jiale Zhang, Junjun Chen, Di Wu, Bing Chen, and Shui Yu. 2019. Poisoning attack in federated learning using generative adversarial nets. In *2019 18th IEEE international conference on trust, security and privacy in computing and communications/13th IEEE international conference on big data science and engineering (TrustCom/BigDataSE)*. IEEE, 374–380.
- [38] Lin Zhang, Li Shen, Liang Ding, Dacheng Tao, and Ling-Yu Duan. 2022. Fine-tuning global model via data-free knowledge distillation for non-iid federated learning. In *Proceedings of the IEEE/CVF conference on computer vision and pattern recognition*. 10174–10183.
- [39] Yanlin Zhou, George Pu, Xiyao Ma, Xiaolin Li, and Dapeng Wu. 2020. Distilled one-shot federated learning. *arXiv preprint arXiv:2009.07999* (2020).
- [40] Zhuangdi Zhu, Junyuan Hong, and Jiayu Zhou. 2021. Data-free knowledge distillation for heterogeneous federated learning. In *International conference on machine learning*. PMLR, 12878–12889.

A More Performance Overview Results on MNIST and SVHN

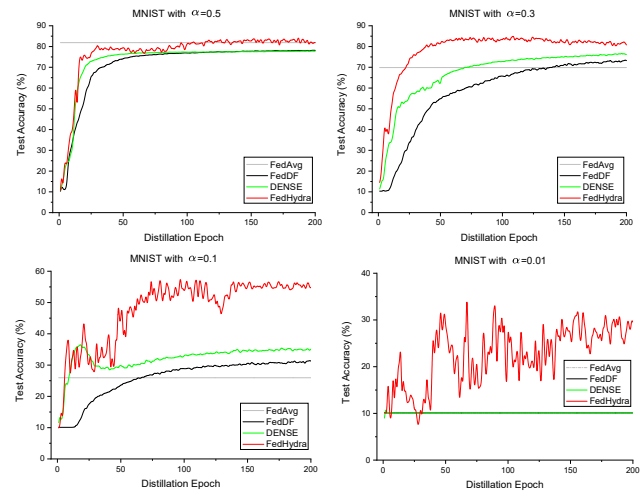


Figure 10: Test accuracy versus distillation epoch over MNIST with $\alpha = \{0.5, 0.3, 0.1, 0.01\}$.

Fig. 10 shows the curves of accuracy versus distillation epoch over MNIST with $\alpha = \{0.5, 0.3, 0.1, 0.01\}$, the results show that FedHydra overtakes other baseline methods after round 15 epochs, and the proposed FedHydra fluctuates but still can reach the peak at 60 epochs around 35.00% when $\alpha = 0.01$, while others keep the performances as 10%.

On the SVHN dataset, FedHydra outperforms other baseline methods after 50 epochs as shown in Fig. 11. Additionally, FedHydra shows a dithering upward trend and peaks around 60 epochs when $\alpha = 0.01$.

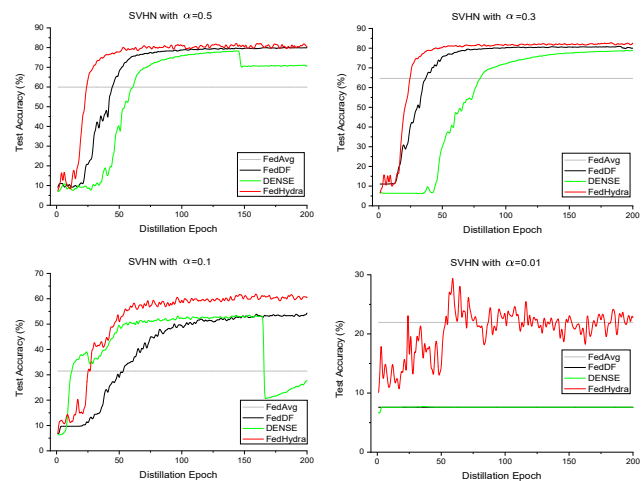


Figure 11: Test accuracy versus distillation epoch over SVHN with $\alpha = \{0.5, 0.3, 0.1, 0.01\}$.

Table 4: Top-1 test accuracy achieved by FedAvg, FedDF, DENSE, and FedHydra over SVHN and CIFAR10 with different client numbers $K = \{5, 10, 20, 50, 100\}$.

Client	SVHN				CIFAR10			
	FedAvg	FedDF	DENSE	FedHydra	FedAvg	FedDF	DENSE	FedHydra
5	59.94	80.20	79.44	82.39	38.26	54.81	58.48	63.15
10	43.45	70.20	69.51	77.13	41.71	50.17	55.43	61.58
20	47.87	69.36	69.10	76.54	33.47	38.70	42.50	59.64
50	36.77	68.30	67.74	74.89	31.75	37.85	39.09	52.66
100	23.69	50.37	48.87	60.01	27.23	33.90	36.25	47.40

B Extended Analysis

B.1 Impact of Client Numbers

Furthermore, we also test the impact of client numbers on SVHN and CIFAR10 by varying the numbers of clients $K = \{5, 10, 20, 50, 100\}$, as shown in Table 4. All the methods decrease when the client number increases. However, FedHydra has less impact than other methods, which achieves 60.01% when $K = 100$ and outperforms the second-best FedDF with only 50.37% on the SVHN dataset. The same trends are shown on the CIFAR-10 dataset. FedHydra achieves 47.40% when $K = 100$ and outperforms the second-best DENSE with only 36.25%. Thanks to the proposed SA algorithm, FedHydra minimally affects the increase in clients.

B.2 Performance Under Multiple Global Training Rounds

We extend our experiments to multiple global rounds. Specifically, we fix the local epoch $E = 50$ and $\alpha = 0.1$ to evaluate the performance of diverse methods on SVHN and CIFAR10 with varying client distributions. Table 5 summarizes the relevant evaluation results. The results in Table 5 show that FedHydra outperforms the other methods with different global training rounds from $T = \{1, 2, 3, 4, 5\}$. In SVHN, the performance of FedHydra steadily increases and reaches a peak when $T = 3$, which outperforms DENSE by 1.86%. In CIFAR-10, FedHydra still performs better than other methods, which keeps steady after $T = 2$ and overtake the second-best FedAvg by 9.2%.

Table 5: Top-1 test accuracy achieved by FedAvg, FedDF, DENSE, and FedHydra over SVHN and CIFAR10 with $\alpha = 0.1$ under multiple global rounds.

Global round	SVHN				CIFAR10			
	FedAvg	FedDF	DENSE	FedHydra	FedAvg	FedDF	DENSE	FedHydra
$T=1$	28.31	48.13	48.22	53.27	22.72	21.33	29.60	37.95
$T=2$	34.55	56.62	54.67	59.98	37.32	28.63	32.39	46.52
$T=3$	44.60	65.61	68.44	70.30	35.95	30.36	36.42	48.75
$T=4$	57.05	63.62	66.83	68.58	43.86	30.71	38.85	50.17
$T=5$	61.59	66.66	64.57	70.39	41.99	28.82	37.27	49.34

B.3 Visualization of Synthetic Data

To assess how synthetic data compares to actual training data, we provide the image comparison between the original training data and synthetic data on FashionMNIST and CIFAR-10 in Fig. 12. The

**Figure 12: Visualization of synthetic data generated by the generator about FashionMNIST and CIFAR10.**

figure demonstrates that the first and third rows display the original data from FashionMNIST and CIFAR10, respectively. In contrast, the second and last rows showcase the synthetic data produced by models trained on the FashionMNIST and CIFAR-10 datasets. Notably, the synthetic data differ significantly from the original data, effectively minimizing the risk of exposing sensitive client information. Despite the marked visual differences, the synthetic data contribute to our method outperforming other baseline approaches in performance. This highlights that synthetic data should ideally be easily distinguishable from real data while supporting superior model training outcomes.

C More Experiment Results on SVHN in Heterogeneous FL

Table 6 provides the test results on SVHN in heterogeneous FL. The results show that FedHydra achieves 71.29% when $\alpha = 0.5$, outperforming the second-best FedDF with 69.75%. However, when data heterogeneity increases, FedHydra still has 54.33% while FedDF decreases to 43.82%.

Table 6: Top-1 test accuracy achieved by FedDF, DENSE, and FedHydra over SVHN with personalized client models.

Data Distribution	Personalized Client Model					Server (ResNet18)		
	GoogLeNet	ResNet18	CNN1	CNN2	LeNet	FedDF	DENSE	FedHydra
$\alpha=0.01$	24.17	7.59	29.81	34.76	19.52	43.82	42.39	54.33
$\alpha=0.1$	42.28	14.84	39.64	34.80	31.17	37.43	36.00	47.45
$\alpha=0.3$	66.78	65.62	38.22	58.73	64.19	77.22	75.75	77.52
$\alpha=0.5$	72.54	70.72	39.74	69.24	64.56	69.75	64.67	71.29

Table 7 summarizes the extra test results on SVHN and CIFAR10 with $2c/c$ in heterogeneous FL. We observe that the performance of all the client models is relatively low under the $2c/c$ setting, while FedDF and DENSE can only achieve 24.72% and 20.42% on SVHN, respectively. However, FedHydra still can reach 31.22, which overpasses the FedDF 6.5%. The same results are shown on

Table 7: Top-1 test accuracy achieved by FedDF, DENSE, and FedHydra over SVHN and CIFAR10 with 2c/c in heterogeneous OFL.

Dataset with 2c/c	Personalized Client Model					Server (ResNet18)		
	GoogLeNet	ResNet18	CNN1	CNN2	LeNet	FedDF	DENSE	FedHydra
SVHN	25.78	26.30	18.48	15.13	11.85	24.72	20.42	31.22
CIFAR10	19.43	18.10	18.69	19.62	19.00	31.05	26.18	38.57

Table 8: Top-1 test accuracy achieved by FedAvg, FedDF, DENSE, and FedHydra over SVHN and CIFAR10 with $\alpha = 0.5$ under multiple global rounds.

Dataset Global round	SVHN				CIFAR10			
	FedAvg	FedDF	DENSE	FedHydra	FedAvg	FedDF	DENSE	FedHydra
T=1	58.88	80.55	79.50	84.97	38.26	48.14	50.23	53.48
T=2	71.36	84.22	82.88	85.37	41.71	49.26	52.58	57.09
T=3	85.73	85.76	84.21	86.41	45.42	48.71	55.39	62.75
T=4	84.12	85.04	83.53	86.46	49.81	48.86	53.81	61.83
T=5	83.84	85.20	84.60	86.81	51.75	49.70	53.49	64.71

CIFAR-10, FedHydra reaches 38.57 which overpasses the FedDF 7.52%

D More Experiment Results Under Multiple Global Rounds Across Diverse α Values

Table 8, 9, 10, and 11 provide the relevant test results with $\alpha = \{0.5, 0.3, 0.01\}$ and 2c/c under five global rounds.

Table 8 shows that the proposed FedHydra outperforms and is more stabilized than all the other methods from different global rounds when $\alpha = 0.5$. The performance of FedHydra keeps above 80% on SVHN and outperforms the best second method 2% to 3%. The gap is much higher on CIFAR-10, where FedHydra can outperform more than 10%, compared with the second-best DENSE on the 5th global round. Table 9 presents that FedHydra consistently outperforms the other methods on both datasets, demonstrating a marked advantage, particularly on the more complex CIFAR10 dataset. For instance, it peaks at 86.72% on SVHN and 58.43% on CIFAR-10, significantly higher than its competitors. The α is set to 0.01 on Table 10, FedHydra consistently outperforms the other algorithms across all rounds and both datasets, demonstrating exceptional adaptability and robustness under high data heterogeneity. Specifically, FedHydra's accuracy peaks at 39.58% on SVHN and 39.76% on CIFAR10, significantly surpassing the next-best results from other models.

Table 9: Top-1 test accuracy achieved by FedAvg, FedDF, DENSE, and FedHydra over SVHN and CIFAR10 with $\alpha = 0.3$ under multiple global rounds.

Dataset Global round	SVHN				CIFAR10			
	FedAvg	FedDF	DENSE	FedHydra	FedAvg	FedDF	DENSE	FedHydra
T=1	61.17	77.99	76.76	79.14	33.72	37.56	41.54	50.01
T=2	73.50	84.21	82.68	84.83	37.56	38.94	46.44	57.00
T=3	84.29	84.49	84.81	85.56	36.04	40.73	47.10	58.18
T=4	84.13	85.04	83.82	86.02	41.73	41.10	46.20	58.43
T=5	84.96	85.89	84.62	86.72	44.26	41.03	48.55	55.97

Table 10: Top-1 test accuracy achieved by FedAvg, FedDF, DENSE, and FedHydra over SVHN and CIFAR10 with $\alpha = 0.01$ under multiple global rounds.

Dataset Global round	SVHN				CIFAR10			
	FedAvg	FedDF	DENSE	FedHydra	FedAvg	FedDF	DENSE	FedHydra
T=1	19.60	7.59	7.59	29.58	10.00	14.39	23.84	30.13
T=2	20.10	7.59	7.59	27.75	17.77	14.89	24.84	37.67
T=3	19.58	7.59	19.77	31.73	26.02	16.42	27.24	39.76
T=4	28.58	7.59	9.86	30.98	25.57	16.79	29.16	38.17
T=5	21.73	7.59	8.04	39.58	27.68	17.59	26.04	38.30

Table 11: Top-1 test accuracy achieved by FedAvg, FedDF, DENSE, and FedHydra over SVHN and CIFAR10 with 2c/c under multiple global rounds.

Dataset Global round	SVHN				CIFAR10			
	FedAvg	FedDF	DENSE	FedHydra	FedAvg	FedDF	DENSE	FedHydra
T=1	26.40	24.51	35.57	49.30	12.23	17.84	23.57	28.34
T=2	36.37	36.00	29.54	57.35	15.62	18.61	22.05	25.54
T=3	30.00	54.43	43.53	62.45	16.10	16.76	25.97	32.25
T=4	39.56	58.41	38.65	59.58	20.44	15.81	20.06	35.69
T=5	34.53	57.12	34.52	65.76	18.24	17.28	24.24	38.76

Table 11 assesses the performance under a 2c/c setting across five global training rounds. FedHydra consistently outshines the other algorithms in both datasets, showing its superior adaptability and robustness, with peak accuracies reaching 65.76% on SVHN and 38.76% on CIFAR10 by the fifth round. FedDF generally performs well on SVHN, albeit less consistently on CIFAR10, while DENSE exhibits mixed results across rounds and datasets. FedAvg consistently underperforms, highlighting its limitations in more complex or skewed data environments. Overall, FedHydra emerges as the most effective method, particularly adept at handling challenges presented by the 2c/c setting, suggesting strong capabilities in managing diverse and complex data distributions in federated learning scenarios. These results underscore FedHydra's potential effectiveness in federated learning scenarios where managing diverse data distributions is critical, marking it as a superior choice in handling complex data heterogeneity challenges in federated environments.

E Comparison with More Conventional Parameter Aggregation Methods

Due to the design rationale behind multi-round optimization, most conventional federated aggregation algorithms are not directly applicable to one-shot FL scenarios. In our study, we also evaluate neuron-matching based model aggregation, such as the OT algorithm [28], in multi-round FL as a representative baseline to be applied to one-shot FL with the same model architecture. The experimental results presented in Table 12 demonstrate that our proposed FedHydra outperforms OT and the other three baselines. Although OT performs better than FedAvg, it generally lags behind FedDF. Furthermore, the neuron-matching based aggregation mechanism employed in multi-round FL is not able to handle the model heterogeneity issue in one-shot FL, which significantly limits its applicability in practical FL scenarios.

Table 12: Top-1 test accuracy achieved by diverse methods over MNIST and CIFAR10 with varying α .

Dataset	MNIST				CIFAR10			
Method	$\alpha=0.5$	$\alpha=0.3$	$\alpha=0.1$	$\alpha=0.01$	$\alpha=0.5$	$\alpha=0.3$	$\alpha=0.1$	$\alpha=0.01$
FedAvg	68.47	54.09	14.39	10.10	43.72	34.78	29.52	11.71
FedDF	71.98	63.00	31.62	10.36	58.97	54.93	38.49	18.84
OT	69.74	59.37	24.05	15.47	46.17	37.63	29.54	22.00
DENSE	70.64	65.79	37.41	14.24	57.78	54.81	48.20	30.34
FedHydra (ours)	78.42	75.80	61.27	43.68	66.83	62.86	55.48	39.99

F Time Complexity Analysis

Here, we briefly compare the time complexity analysis between our FedHydra algorithm and DENSE, the primary baseline. Assume that the time complexity (TC) of completing one batch training round of generator is $O(1)$. Without considering the TC of the global model training, the total TC for DENSE is $O(T_g \cdot T_G)$ while for our FedHydra it is $O((m \cdot c + T_g) \cdot T_G)$. Considering the computation capability of the central server and limited client numbers m and classes c , we believe the increased TC of $O(m \cdot c \cdot T_G)$ is acceptable in practical FL applications when comparing between FedHydra and DENSE. The results of five repeat experiments with running time (seconds) on CIFAR10 are

FedHydra: [5540.096, 5690.33, 5661.529, 5633.972, 5594.553]

DENSE: [5177.561, 5327.501, 5097.391, 5267.725, 5127.312]

showing that FedHydra is approximately 7% higher than DENSE.

G Details of Dataset

The MNIST [13] dataset is a foundational resource in machine learning, specifically for computer vision tasks, consisting of 70,000 handwritten digit images used to train and test image recognition algorithms. It is divided into a training set of 60,000 examples and a test set of 10,000 examples, with each image being a 28x28 pixel grayscale representation of digits 0 through 9. MNIST serves as a benchmark for evaluating the performance of machine learning models. Despite its simplicity, MNIST is critically acclaimed for its role in advancing machine learning techniques.

Fashion-MNIST [33] is an advanced dataset introduced as an alternative to the original MNIST, aimed at providing a greater challenge for machine learning models in image classification. Developed by Zalando, it comprises 70,000 grayscale images of fashion items categorized into 10 types, such as T-shirts, trousers, and sneakers, divided into a training set of 60,000 and a test set of 10,000 images. Designed to be a direct replacement for MNIST, Fashion-MNIST maintains the same format and size, encouraging more sophisticated modeling techniques without requiring significant computational resources, thus making it suitable for benchmarking purposes.

The Street View House Numbers (SVHN) [22] dataset is a complex, real-world image dataset derived from Google Street View images, designed for machine learning tasks like digit recognition. It contains over 600,000 digit images, offering a substantial challenge due to its size and the real-life variability of its images, including differences in lighting, digit styles, and background clutter. SVHN is structured into two formats: the first includes full numbers with bounding boxes for digit localization, while the second focuses on images centered around single digits for classification tasks. This dataset is particularly valued for testing the robustness of machine

learning models, such as convolutional neural networks, in recognizing numbers under varied and realistic conditions.

The CIFAR-10 [12] dataset, established by the Canadian Institute for Advanced Research, is a fundamental benchmark for machine learning and computer vision research, focusing on object recognition tasks. It comprises 60,000 color images of 32x32 pixels each, evenly distributed across 10 classes - airplanes, cars, birds, cats, deer, dogs, frogs, horses, ships, and trucks. With a division of 50,000 images for training and 10,000 for testing, CIFAR-10 challenges algorithms with its real-world variability, including diverse object orientations, varied backgrounds, and fluctuating lighting conditions. This dataset represents a moderate step up in complexity from introductory datasets like MNIST, providing a balanced platform for testing and refining advanced image recognition models, especially convolutional neural networks, within a controlled yet realistic setting.